Structure of Adsorbed Polymer Layers: Molecular Volume Effects

Harry J. Ploehn

Department of Chemical Engineering, Texas A&M University, College Station, Texas 77843-3122

Received June 18, 1993; Revised Manuscript Received November 30, 1993•

ABSTRACT: A new continuum model for homopolymer adsorption is developed within the framework of self-consistent field theory. The model differs from previous lattice-based and continuum models in that it properly accounts for polymer stiffness in the idealization of a polymer molecule as a chain of segments and it allows segments and solvent molecules to have differing partial molar volumes. The altered balance of mixing enthalpy and entropy has quantitative implications for the structure of adsorbed polymer layers. Beginning with a heuristic development of a free energy balance for the system, functional minimization of the free energy determines the appropriate form of the self-consistent field. The field appears in a modified diffusion equation which governs the spatial distribution of polymer. This equation is solved via a regular perturbation expansion in powers of reciprocal polymer molecular weight. Retention of only the first term precludes tails but allows a semianalytical solution. We explore the effects of varying polymer–solvent interactions and partial molar volumes upon adsorbed layer structure, and we compare predicted polymer adsorbed masses and layer thicknesses with experimental values.

I. Introduction

The methods of statistical mechanics,[1] combined with dimensional analysis principles embodied in scaling concepts,[2] have engendered considerable understanding of structure–property relationships in bulk polymers, polymer blends, polymer solutions, and polymers localized at phase boundaries. Elucidation of structure–property relationships in polymer interphases[3] is particularly challenging for two reasons: the structures of interest are spatially inhomogeneous, and their length scales are typically much smaller than macroscopic dimensions. The task necessitates the development of new experimental techniques capable of resolving inhomogeneous structures on molecular length scales, and the refinement of microstructural models which accommodate spatial variations of the material's intensive properties. The experimental challenge has been met by techniques such as neutron and X-ray scattering, surface imaging via atomic force and scanning tunneling microscopy, and direct surface forces measurements. The continuing evolution of theoretical models is motivated by the need to rationalize increasingly detailed experimental data.

Models of microstructure in polymer interphases often utilize the tools of statistical mechanics. The partition function plays a pivotal role by connecting the detailed, molecular-level description of the configuration of a system with its thermodynamic properties. Complications arise, however, in describing the configurations of polymer molecules, in accounting for the energy effects of interactions between components, and in minimizing the free energy of the system to determine its equilibrium state. Various polymer interphase models handle these issues in differing ways,[2,4] reflecting different approaches to achieving qualitative and quantitative accuracy while maintaining mathematical tractability.

Two distinct classes of statistical mechanical models of polymer interphases have emerged from a large body of early theoretical development:[4] "square-gradient" (SG) theory (or the "Cahn-de Gennes" approach) and self-consistent field (SCF) theory. The SG and SCF theories are mathematically equivalent if the probability of finding a segment of a polymer chain at a given location is independent of the rank of the segment in the chain, i.e. in the limit of infinite polymer molecular weight. Both theories require, as input, an equation of state which quantifies the free energy density associated with interactions of components at a specified location.

SG models are based on the Cahn–Hilliard[5] theory for predicting the free energy of interphases containing small molecules. The free energy of the interphase is written as a integral of the free energy density over the corresponding spatial domain. The integrand is expanded in powers of composition gradients with the series truncated at the square-gradient term. The first term in the series is the free energy density of a (perhaps hypothetical) homogeneous mixture evaluated at the local composition. The positive square-gradient term represents the energy penalty associated with maintaining the inhomogeneity of the interphase. Although the coefficient of the square-gradient term was initially treated as a phenomenological parameter, more recent developments[5] provide a statistical mechanical foundation for its composition dependence. de Gennes[6] adapted SG theory to describe the free energy and interactions of adsorbed polymer layers; subsequent refinements[7–9] for a variety of solution conditions sought to rationalize concurrent surface forces data.[10]

Although SG theory employs relatively straightforward mathematics and gives reasonable qualitative predictions, it cannot provide detailed information on molecular configurations within polymer interphases. At the expense of greater computational effort, SCF theory can provide additional microstructural information. SCF theory constructs an expression for the free energy, via the partition function, from the configurations of constituent molecules. A coarse-graining procedure[11] transforms the description based on detailed configurations into one utilizing continuous component density distributions. After expansion of the total "site–site" interaction potential energy in powers of composition gradients and truncation at the pair interaction level, free energy minimization provides an equilibrium relationship which fixes the spatial distribution of components in the interphase.

SCF theories can be classified by their manner of representing the partition function. Lattice models, exemplified by that of Scheutjens and Fleer,[12] represent space as a set of discrete lattice cells of constant volume. In a finite domain, and for a specified overall composition, the number of possible configurations of the constituent

• Abstract published in *Advance ACS Abstracts*, February 1, 1994.

0024-9297/94/2227-1617$04.50/0

molecules is finite. The total intermolecular potential energy is assumed to be the sum of pair interactions. Thus the partition function takes the form of a sum of Boltzmann factors weighted by combinatory prefactors which characterize the degeneracy of states.

Alternately, the configurations of polymer molecules may be idealized as space curves.[13] The partition function can then be written as a functional integral over the domain of configuration space with the integrand a Boltzmann factor depending on the total intermolecular potential energy. The expansion of potential energy in powers of composition gradients with appropriate truncation is equivalent to the assumption of pair interactions. Free energy minimization is accomplished through methods of variational calculus,[14] yielding the equilibrium structure in terms of continuous density distributions.

Lattice and continuum versions of SCF theory differ in the way that space is filled with molecules. Most lattice models stipulate that every lattice cell must be occupied by either a solvent molecule or a polymer segment. Hence a polymer segment must have the same volume as a solvent molecule. From the cell volume, the bulk density of the polymer, and its degree of polymerization, the number of segments per polymer molecule is readily determined. However, the result does not reflect the intrinsic stiffness of the polymer molecule represented by a parameter such as the characteristic ratio, C_∞, or the radius of gyration in a theta solvent, R_g.

Continuum models require that the volume fractions of all components sum to unity at all points. This constraint can be imposed through a virtual compressibility term in the free energy density[15] or by incorporating the constraint in the partition function via a Lagrange multiplier.[11] Issues of compressibility and differing molecular volumes are therefore separated from the problem of idealizing real polymer molecules as chains of segments. By equating the extended contour lengths and radii of gyration of real molecules and chains of segments, we fix the number of segments per chain and the equivalent length of a segment. If the segment length is small compared to the total contour length, the chain is essentially a continuous space curve, i.e. a random walk of "differential" freely-jointed segments.

The differences between lattice and continuum SCF models affect the calculation of the free energy density in polymer solutions and interphases. The energy of mixing polymer and solvent depends on the number of solvent–monomer contacts, but the entropy of mixing depends on the numbers of independent kinetic units, i.e. solvent molecules and segments. Since lattice and continuum models differ in choice of molecular volumes and number of monomers per segment, we expect quantitative differences when comparing model predictions with experimental data.

In this paper, we will explore the effects of incompressibility and molecular volume differences upon the structure of adsorbed polymer layers. We describe a continuum-based SCF model which incorporates these effects in the free energy density via an extended form of the Flory–Huggins equation of state.[16] The foundations for this model are provided by the work of Edwards,[13] who first recognized the analogy between a polymer configuration and the trajectory of a particle moving in a potential field, by Helfand,[15] who formalized the use functional integrals for describing polymer interphases, and by Hong and Noolandi,[11] who completed the development of a rigorous statistical mechanical theory. References to these works obviate the need for a more detailed review of the statistical mechanics here.

Instead, we will pursue a heuristic development similar to that of Evans and Needham[17] which will hopefully provide additional insight. In particular, we will illustrate some of the salient features of the SCF model through further analogies between established statistical mechanical forms and descriptions provided by classical thermodynamics and continuum mechanics. We begin by constructing a free energy balance for a multicomponent mixture occupying two distinct regions: homogeneous bulk solution and an inhomogeneous interphase generated by an adsorbing surface. We postulate the existence of "extra" potential energy fields which maintain the inhomogeneity of the interphase. Functional minimization of the free energy establishes an equilibrium relationship which determines the composition dependence of the extra potential fields. We then determine the spatial distributions of components in the interphase by solving the self-consistent field equations via a regular perturbation expansion in powers of reciprocal polymer molecular weight. We limit our analysis to the "ground state" solution, precluding tail configurations but enabling semianalytical calculations.

We subsequently explore the qualitative effects of polymer–solvent interactions and molecular volume differences upon adsorbed layer structure. In addition, model predictions for the polymer adsorbed mass per area and adsorbed layer thickness are compared with experimental data. In a subsequent publication,[18] we analyze the stress and work per area for compression of adsorbed polymer layers using fundamental conservation postulates. In that report, we also present comparisons of predicted compression work with experimental surface forces data.

II. Thermodynamics of Inhomogeneous Interphases

A. Continuum Model of an Interphase. Consider a multicomponent mixture of n components labeled $k = 1, ..., n$. The domain of the system containing this mixture includes a spatially homogeneous "bulk" region (superscript b) and an interphase[3] in which the mixture's intensive properties are spatially inhomogeneous. The temperature, total numbers of moles of each component, and partial molar volumes of each component (T, N_k, and $\bar{V}_k$, respectively) are assumed constant; consequently, the total volume of the system is also constant. For polymeric components, N_k is the number of moles of monomers and $\bar{V}_k$ is the volume per mole of monomers.

The system is closed with respect to exchange of mass and thermal energy with the surroundings, but the system is assumed to be in mechanical equilibrium with the surroundings at a pressure P^b. The total volume of the bulk region is V^b. We denote N_k^b and μ_k^b as the number of moles and the chemical potential (partial molar Gibbs free energy) of component k in the bulk region. We suppose that the interphase occupies a region near a planar surface which forms part of the system boundary. The area of the surface is A_s and, with z as the normal coordinate direction, the thickness of the interphase is denoted as z_m. The value of z_m is arbitrary insofar as the local intensive properties at that distance from the surface are the same as those of bulk solution. We assume that the local intensive properties in the interphase, including component molar densities, pressure, and free energy density, are uniform in directions parallel to the surface.

We have tacitly assumed that the intensive properties of the mixture are continuous in bulk solution as well as in the interphase. Underlying this assumption are two fundamental postulates. First, the ensemble postulate of

statistical mechanics equates the ensemble average of any mechanical property of the system with the corresponding thermodynamic property.[19] Second, a form of the continuum hypothesis enables the representation of interphase material properties as continuous functions if the length scale of inhomogeneity is much greater than the range of intermolecular forces.[20] This hypothesis is implicit in the Kirkwood–Buff theory of surface tension[21] as well as lattice-based[12] and continuum[11,15–17] SCF theories. Under these conditions, the model of the interphase as an inhomogeneous continuum is consistent with parallel statistical mechanical descriptions.

B. Equilibrium Energy Balance. Having established our view of the interphase as an inhomogeneous continuum, we suppose that it merges continuously into bulk solution with the distance z_m an arbitrary point of demarcation. The heuristic development[17] of SCF thermodynamics postulates that the total Helmholtz free energy of the system is

$$A = -P^b V^b + \sum_k N_k{}^b \mu_k{}^b + A_s \int_0^{z_m} [\sum_k (\mu_k{}^H - \epsilon_k)\rho_k - P]\, dz \quad (1)$$

where the integral term is the Helmholtz free energy of material in the interphase. The chemical potential of component k in the interphase, $(\mu_k{}^H - \epsilon_k)$, is the sum of a local contribution, $\mu_k{}^H$, evaluated as though the mixture were homogeneous at the local composition, plus a nonlocal contribution, $-\epsilon_k$, arising from the spatial inhomogeneity. It is helpful to view ϵ_k as an "extra" potential energy field which maintains the inhomogeneous density distribution of component k. The local pressure in the interphase is P, and

$$N_k - N_k{}^b = A_s \int_0^{z_m} \rho_k\, dz \quad (2)$$

defines ρ_k, the local molar density of component k in the interphase.

The fields ϵ_k are to be selected so that $\rho_k(z)$ is an equilibrium distribution consistent with configurational constraints imposed by polymer chain connectivity. For any component not subject to configurational constraints, such as solvent, the field ϵ_k is identically zero.

An equilibrium condition is determined by minimizing the system's free energy while holding T, $\bar{V}_k$, N_k, A_s, and z_m constant. Taking variations of eq 1 gives

$$\delta A = \sum_k N_k{}^b \delta\mu_k{}^b + \sum_k \mu_k{}^b \delta N_k{}^b - P^b \delta V^b - V^b \delta P^b + A_s \int_0^{z_m} (\delta[\sum_k (\mu_k{}^H - \epsilon_k)\rho_k - P] + \zeta \sum_k \bar{V}_k \delta\rho_k)\, dz \quad (3)$$

which incorporates the constraint $\sum_k \bar{V}_k \delta\rho_k \equiv 0$ (since the volume fractions $\bar{V}_k\rho_k$ must sum to unity at all points) through the Lagrange multiplier $\zeta(z)$. The first and fourth terms on the right side of eq 3 sum to zero since, for the bulk region, the volume is $V^b = \sum_k N_k{}^b \bar{V}_k$ and the Gibbs–Duhem equation provides $\bar{V}_k = (\partial\mu_k{}^b/\partial P^b)_{T,N_j}$. Variations in the volume and composition of the bulk region are related by $\delta V^b = \sum_k \bar{V}_k \delta N_k{}^b$ so that the second and third terms of eq 3 become

$$\sum_k \mu_k{}^b \delta N_k{}^b - P^b \delta V^b = \sum_k (\mu_k{}^b - \bar{V}_k P^b)\delta N_k{}^b \quad (4)$$

where $\mu_k{}^b - \bar{V}_k P^b$ represents a partial molar Helmholtz free energy. Constant N_k implies

$$\delta N_k = 0 = \delta N_k{}^b + A_s \int_0^{z_m} \delta\rho_k\, dz \quad (5)$$

which may be used to eliminate $\delta N_k{}^b$ in eq 3. With these simplifications, eq 3 becomes

$$\delta A = A_s \int_0^{z_m} [\delta[\sum_k (\mu_k{}^H - \epsilon_k)\rho_k - P] - \sum_k (\mu_k{}^b - \bar{V}_k P^b - \zeta\bar{V}_k)\delta\rho_k]\, dz \quad (6)$$

after using the identity $P = \sum_k \bar{V}_k P \rho_k$.

The leading term on the right side of eq 6 can be simplified by requiring that the Gibbs–Duhem equation be satisfied at each point in the interphase so that $\delta(\mu_k{}^H - \epsilon_k - \bar{V}_k P^b) = 0$. Equation 6 then becomes

$$\delta A = A_s \int_0^{z_m} \{\sum_k [\mu_k{}^H - \mu_k{}^b + \zeta\bar{V}_k - \epsilon_k]\delta\rho_k\}\, dz \quad (7)$$

We establish an equilibrium condition by setting $\delta A \equiv 0$ for all variations at constant A_s and z_m. The resultant expression for the equilibrium self-consistent field

$$\epsilon_k = \mu_k{}^H - \mu_k{}^b + \zeta\bar{V}_k \quad (8)$$

agrees with prior statistical mechanical theories.[11–17] Solvent molecules are taken to have no configurational degrees of freedom, so eq 8 with $\epsilon_s \equiv 0$ determines the Lagrange multiplier as

$$\zeta(z) = -\frac{(\mu_s - \mu_s{}^b)}{\bar{V}_s} \equiv \Pi(z) - \Pi^b \quad (9)$$

with the second equality utilizing the definition of the osmotic pressure. Combining eqs 8 and 9 produces

$$\epsilon_k = \mu_k{}^H - \mu_k{}^b - \frac{\bar{V}_k}{\bar{V}_s}(\mu_s{}^H - \mu_s{}^b) = \mu_k{}^H - \mu_k{}^b + \bar{V}_k(\Pi - \Pi^b) \quad (10)$$

as the final expression for the "extra" potential energy field. The magnitude of ϵ_k depends critically upon the relative partial molar volumes of components k and solvent. The "extra" potential energy is zero in the homogeneous bulk region.

Rearrangement of eq 10 produces an expression of phase equilibrium

$$\mu_k{}^H - \epsilon_k + \bar{V}_k\Pi = \mu_k{}^b + \bar{V}_k\Pi^b \quad (11)$$

with the osmotic pressure interpreted as an additional potential which maintains the constraint of incompressibility at all points in the system. This is an example of generalized "membrane" equilibrium as discussed by Lyklema.[22] Alternately, equilibrium can be expressed[17] in terms of transfer chemical potentials defined by $\bar{\mu}_k \equiv \mu_k{}^H - (\bar{V}_k/\bar{V}_s)\mu_s{}^H$ so that $\bar{\mu}_k - \epsilon_k = \bar{\mu}_k{}^b$. Hence the transfer chemical potential in the interphase $(\bar{\mu}_k - \epsilon_k)$ equals that in the bulk phase at equilibrium.

Substitution of eqs 8 and 9 into eqs 1 and 2 leads to the correct form[22] of the total Helmholtz free energy

$$A = -P^b V + \sum_k N_k \mu_k{}^b + A_s\gamma \quad (12)$$

with the surface tension given by the Kirkwood–Buff form[21]

$$\gamma = \int_0^{z_m} [\Pi^b - \Pi(z)]\, dz \tag{13}$$

in agreement with all previous SG and SCF theories.[4-9,11-18,20]

C. Constrained Equilibrium. In many cases of practical interest, the distributions of some of the components are restricted by additional constraints. For example, transport of polymer molecules into or out of the interphase may be hindered by diffusive or convective limitations. The simplest way to handle this situation is to assume that the number of moles of a restricted component k in the interphase remains constant over time scales of experimental interest. We thus require

$$\delta[A_s \int_0^{z_m} \rho_k\, dz] = A_s \int_0^{z_m} \delta\rho_k\, dz = 0 \tag{14}$$

for each restricted component and for all variations that do not change the shape of the interphase.

This constraint is imposed[17] by adding the product of eq 14 with a Lagrange multiplier, g_k, to the free energy variational statement, eq 3. Of course, g_k is identically zero if component k is not restricted. Minimization of the free energy proceeds in the same manner as for the full equilibrium case presented above. Again, we identify an equilibrium expression by requiring $\delta A \equiv 0$ for all variations which do not change the shape of the interphase, producing

$$\epsilon_k = \mu_k^H - \mu_k^b + \zeta \bar{V}_k + g_k \tag{15}$$

as found by Evans and Needham.[17] Since the exchange of solvent between bulk and interphase is not constrained, we require $g_s \equiv 0$ as well as $\epsilon_s \equiv 0$, so eq 9 again fixes $\zeta(z)$. Equations 9 and 15 thus determine

$$\mu_k^H - \epsilon_k + g_k + \bar{V}_k \Pi = \mu_k^b + \bar{V}_k \Pi^b \tag{16}$$

as the equilibrium expression for interphases containing constrained components.

Substitution of eq 16 into eqs 1 and 2 produces eq 12 for the total Helmholtz free energy with

$$\gamma = \int_0^{z_m} [\Pi^b - \Pi(z) - \sum_k g_k \rho_k]\, dz \tag{17}$$

for the surface tension.

We can view the Lagrange multipliers g_k in at least two ways. The interphase can be treated as though it were in equilibrium with a hypothetical bulk solution by combining g_k and μ_k^b into pseudochemical potentials.[6-9,12c] Alternately, the g_k may be regarded as additional potentials that maintain a certain distribution of restricted components between the interphase and bulk solution.[17] Thus g_k is negative when component k must be held in the interphase and positive when it must be prevented from entering the interphase. If we presume the existence of an initial state in which all of the g_k are zero, then the nonzero values of the g_k in some final state depend on the process by which the initial state is transformed into the final state. Since T, V, and N_k, remain constant, we presume that the values of the g_k depend on the details of deformations which move the boundaries of the interphase, i.e. which change A_s or z_m. Analysis of this issue is discussed in detail in a subsequent publication.[18]

III. Self-Consistent Field Theory

In the previous section, we developed a framework for the thermodynamics of a system composed of an inhomogeneous polymeric interphase in equilibrium with a homogeneous polymer solution. In order to determine the structure of single adsorbed polymer layers and to calculate the stress and work per area for compression of two adsorbed layers,[18] we utilize self-consistent field (SCF) theory to model structure within polymeric interphases. We first review the general forms of the governing SCF equations and then we develop a solution for two opposing adsorbed polymer layers using a regular perturbation expansion. Our analysis of the compression of adsorbed polymer layers[18] will utilize "two-surface" solutions for specified values of z_m. For arbitrarily large values of z_m, the solution developed below provides results for a single adsorbed layer.

A. General Field Equations. The statistical mechanical foundation for self-consistent field (SCF) models of inhomogeneous polymeric interphases was established by Edwards,[13] Freed,[14] and Helfand,[15] culminating in the lattice model of Scheutjens and Fleer[12] and the continuum model of Hong and Noolandi.[11] A key intermediate variable which arises an all SCF models is $q(\tilde{r},t)$, the probability density for a chain of t polymer segments that ends at position $\tilde{r}$. Helfand has shown[15] that q satisfies the modified diffusion equation

$$\frac{\partial q}{\partial t} = \frac{l^2}{6} \nabla^2 q - \frac{w_p}{RT} q \tag{18}$$

with initial condition

$$q(\tilde{r},0) = 1 \tag{19}$$

expressing the equal likelihood of chains beginning anywhere. In eq 18, l is the length of a statistical unit, or segment, of a polymer chain, and $w_p(\tilde{r})$ is a "self-consistent" potential energy field defined for a polymeric component.

A field w_k is defined for every component. A probability function q, governed by a modified diffusion equation like eq 18, arises for every polymeric component. Here, we consider mixtures that contain only one polymeric component.

Continuum-based statistical mechanical theories[11,15] determine w_k through functional minimization of the free energy with respect to variations in w_k. The result for nonpolymeric components

$$\rho_s(\tilde{r}) = \frac{1}{\bar{V}_s} \exp\left(-\frac{w_s}{RT}\right) \tag{20}$$

reflects the sole influence of translational (mixing) entropy. For polymeric components with Z_p segments per chain, the polymer density (moles of monomers per volume) is a convolution of the probability density function

$$\rho_p(\tilde{r}) = \frac{1}{\bar{V}_p Z_p} \int_0^{Z_p} q(\tilde{r},t) q(\tilde{r},Z_p - t)\, dt \tag{21}$$

In effect, the polymer volume fraction $\varphi_p \equiv \bar{V}_p \rho_p$ equals the probability of two polymer chain parts having a total of Z_p segments meeting at $\tilde{r}$. The probability functions are normalized so that q is unity and w_k is zero in regions where the molar density ρ_k equals that of pure component k, $1/\bar{V}_k$.

Functional minimization of the free energy with respect to variations in ρ_k requires a functional form for the dependence of the total intermolecular potential on the density distributions. Hong and Noolandi[11] express the total intermolecular potential as an expansion in ρ_k and its spatial gradients. Truncation of the expansion defines a closure, enabling the development of an equilibrium relationship that defines w_k in terms of ρ_k. The free energy

analysis of section II.B is entirely equivalent: the heuristic form of the free energy density, the integral term in eq 1, amounts to a truncation which eliminates all nonlocal gradient terms. Comparison of eq 16 and the form of w_k identified by statistical mechanical theories[11] establishes w_k as[17]

$$w_k = \epsilon_k - \frac{RT}{Z_k}\ln(\bar{V}_k\rho_k) = \mu_k - \mu_k^{\,b} + \bar{V}_k(\Pi - \Pi^b) + g_k - \frac{RT}{Z_k}\ln(\bar{V}_k\rho_k) \quad (22)$$

In a homogeneous region such as a bulk polymer solution, the self-consistent fields are constant and, for polymers, depend on the numbers of segments per chain ($Z_k = 1$ for nonpolymeric components).

B. Regular Perturbation Solution for Adsorbed Polymer Layers. We now consider adsorption of a homopolymer from a polymer–solvent mixture onto two opposing parallel planar surfaces. The surfaces are assumed to be identical and uniform so that intensive properties do not vary in directions parallel to the surfaces. For arbitrarily large values of z_m, we have two isolated adsorbed layers separated by bulk solution. The surfaces are also assumed to be identical so that the structure of the interphase is symmetric about the midplane at $z = z_m$.

Distance from one of the surfaces (z), segment rank (t), and energy are made dimensionless with l, Z_p, and RT, respectively. The self-consistent field equations become

$$\frac{1}{Z_p}\frac{\partial q}{\partial t} = \frac{1}{6}\frac{\partial^2 q}{\partial z^2} - w_p q \quad (23a)$$

$$q(z,0) = 1 \quad (23b)$$

$$\frac{\partial q}{\partial z}(z_m,t) = 0 \quad (23c)$$

$$\frac{\partial \ln q}{\partial z}(0,t) = -\chi_s \quad (23d)$$

$$\bar{V}_p\rho_p = \int_0^1 q(z,t)q(z,1-t)\,dt \quad (23e)$$

where the boundary conditions reflect the homogeneity of bulk solution (eq 23c, z_m large), midpoint symmetry (eq 23c, z_m finite and specified), and the free energy reduction[2,28] χ_s per polymer segment adsorbed in place of a solvent molecule at the surface $z = 0$ (eq 23d).

A semianalytical solution may be obtained by expanding $q(z,t)$ in powers of $1/Z_p$. However, we retain the form of w_p given in eq 22: our normalization (eq 21) and the equilibrium condition (eq 22) demand that w_p depend on Z_p in bulk solution. The lowest order problem in powers of $1/Z_p$ is

$$0 = \frac{1}{6}\frac{d^2 q_0}{dz^2} - w_p q_0 \quad (24a)$$

$$\frac{dq_0}{dz}(z_m) = 0 \quad (24b)$$

$$\frac{d\ln q_0}{dz}(0) = -\chi_s \quad (24c)$$

$$q_0^{\,2} = \bar{V}_p\rho_p = \varphi_p \quad (24d)$$

Equation 24d is used to change variables from q_0 to polymer volume fraction φ_p during the integration of eq 24a.

Keeping only the lowest order term in the expansion of q is equivalent to the ground-state solutions reported previously.[40] In effect, we neglect chain "end effects" upon adsorbed layer structure. This approximation will lead to significant errors at the periphery of the adsorbed layer where the polymer correlation length becomes comparable to the polymer's root-mean-squared end-to-end distance. Since various measures of the thickness of adsorbed polymer layers are known to be sensitive to the distribution of "tails",[12] we should expect poor predictions of layer thicknesses for adsorption from dilute solution in good or Theta solvents. Under these conditions, however, tails make a minor contribution to the total adsorbed mass of polymer. If the polymer concentration in the adsorbed layer lies primarily in the concentrated or semidilute ranges,[4] then we might expect reasonable predictions of the adsorbed mass of polymer per unit area.

To integrate eq 24a, w_p from eq 22 is first written as[15]

$$w_p = \left(\frac{\partial \Delta a}{\partial \rho_p}\right)_{T,P^b,\bar{V}_k} + g_p - \frac{RT}{Z_p}\ln(\bar{V}_p\rho_p) \quad (25)$$

where

$$\Delta a \equiv a_h - (\rho_p\mu_p^{\,b} + \rho_s\mu_s^{\,b} - P^b) \quad (26)$$

defines a mixing free energy density representing the change in the free energy per unit volume for creating a homogeneous region of composition $[\rho_k]$ and free energy density a_h from bulk solution with composition $[\rho_k^b]$. The functional dependence of a_h and μ_k upon $[\rho_k]$ can be obtained from any polymer solution equation of state. We have used an extended form of the Flory–Huggins equation of state which is described in the next section.

Employing eqs 25 and 26, integrating eq 24a, and changing variables via eq 24d produces

$$\left(\frac{d\varphi_p}{dz}\right)^2 = 24\varphi_p[F(\varphi_p,g_p) - F(\varphi_p^{\,m},g_p)] \quad (27)$$

as the first integral with $\varphi_p^{\,m} \equiv \varphi_p(z_m)$ treated as a parameter. The boundary condition 24b defines

$$F(\varphi_p,g_p) \equiv \bar{V}_p\Delta a + g_p\varphi_p + \frac{1}{Z_p}[-\varphi_p\ln(\varphi_p) + \varphi_p^{\,b}\ln(\varphi_p^{\,b}) + \varphi_p - \varphi_p^{\,b}] \quad (28)$$

with an analogous equation for $F(\varphi_p^{\,m},g_p)$. To determine the structure of a single adsorbed layer, we recognize that the polymer volume fraction at the midpoint, $\varphi_p^{\,m}$, approaches the bulk solution value $\varphi_p^{\,b}$, for very large values of z_m. If the adsorbed layer is in full equilibrium with bulk solution, g_p and $F(\varphi_p^{\,m},g_p)$ are identically zero. Thus eq 27 is the first integral of the solution for a single adsorbed layer as well as two interacting adsorbed layers. The second integral of eq 24a

$$z = -\int_{\varphi_0}^{\varphi_p}\frac{du}{\{24u[F(u,g_p) - F(\varphi_p^{\,m},g_p)]\}^{1/2}} \quad (29)$$

gives the polymer volume fraction as an implicit function of the distance from the surface and the surface volume fraction $\varphi_0 \equiv \varphi_p(0)$.

The solution is completely determined by three unknowns, φ_0, $\varphi_p^{\,m}$, and g_p, which depend implicity upon z_m. These unknowns are found from the simultaneous solution of three equations

$$\varphi_0\chi_s^{\,2} - 6F(\varphi_0,g_p) = 0 \quad (30)$$

$$z_m + \int_{\varphi_0}^{\varphi_p^m} \frac{du}{\{24u[F(u,g_p) - F(\varphi_p^m,g_p)]\}^{1/2}} = 0 \quad (31)$$

and

$$\varphi_{ads} + \int_{\varphi_0}^{\varphi_p^m} \frac{(u - \varphi_p^b)\,du}{\{24u[F(u,g_p) - F(\varphi_p^m,g_p)]\}^{1/2}} = 0 \quad (32)$$

which arise from the surface boundary condition 24c, the definition of φ_p^m, and the definition of the dimensionless polymer adsorbed mass φ_{ads}. Equation 32 derives from the more familiar definition

$$\varphi_{ads} = \int_0^{z_m} [\varphi_p(z) - \varphi_p^b]\,dz \quad (33)$$

through the use of eq 27 and the chain rule to change the integration value.

For a single surface, eqs 30–32 are decoupled because $\varphi_p^m = \varphi_p^b$ and $F(\varphi_p^m,g_p)$ is zero under full equilibrium conditions. The structure of the adsorbed layer is determined by the solution of eq 30 for φ_0. Evaluation of eq 31 produces the distance at which the difference $\varphi_p(z) - \varphi_p^b$ decays to a specified tolerance. Equation 32 yields the equilibrium adsorbed mass of polymer. For two interacting adsorbed layers under full equilibrium conditions, eqs 30 and 31 are solved iteratively for a given value of z_m. When the exchange of polymer between the interphase and bulk solution is constrained, we fix φ_{ads} from the single surface equilibrium case. Equations 30–32 are then solved iteratively as a function of z_m.

C. Extended Flory–Huggins Equation of State. Helfand and Sapse[16] introduced an extended form of the Flory–Huggins equation of state which explicitly accounts for volume differences between solvent molecules and monomers. The free energy density, given by

$$a_h = \rho_p\mu_p^\circ + \rho_s\mu_s^\circ - P^\circ + \rho_s \ln(\varphi_s) + \frac{\rho_p}{Z_p}\ln(\varphi_p) + \chi\rho_s\varphi_p \quad (34)$$

is the mixing free energy of creating a homogeneous polymer–solvent mixture from pure components at reference conditions (superscript o). The polymer–solvent interaction parameter is denoted by χ. The usual definitions of the partial molar free energies give

$$\mu_p \equiv \left(\frac{\partial a_h}{\partial \rho_p}\right)_{T,\rho_s} = \mu_p^\circ + \frac{1}{Z_p}\ln(\varphi_p) + \left(\frac{1}{Z_p} - \frac{\bar{V}_p}{\bar{V}_s}\right)\varphi_s + \chi\frac{\bar{V}_p}{\bar{V}_s}\varphi_s^2$$

$$\mu_s \equiv \left(\frac{\partial a_h}{\partial \rho_s}\right)_{T,\rho_p} = \mu_s^\circ + \ln(\varphi_s) + \left(1 - \frac{\bar{V}_s}{\bar{V}_p Z_p}\right)\varphi_p + \chi\varphi_p^2 \quad (35)$$

which reduce to the usual Flory–Huggins forms for equal partial molar volumes. The mixing free energy defined in eq 26 is found to be

$$\bar{V}_p\Delta a = \frac{\varphi_p}{Z_p}\ln\left(\frac{\varphi_p}{\varphi_p^b}\right) + \frac{\bar{V}_p}{\bar{V}_s}\left[\varphi_s \ln\left(\frac{\varphi_s}{\varphi_s^b}\right) + \left(1 - \frac{\bar{V}_s}{\bar{V}_p Z_p}\right)(\varphi_p - \varphi_p^b) - \chi(\varphi_p - \varphi_p^b)^2\right] \quad (36)$$

which is similar to expressions appearing in the lattice model of Scheutjens and Fleer.[12]

Helfand and Sapse[16] identified Z_p as the degree of polymerization, but we use eqs 34–36 with Z_p as the number of segments per polymer chain. Thus the balance of mixing enthalpy and entropy is different in our use of the equation of state from that used previously. The mixing enthalpy is proportional to the number of monomer–solvent contacts, but the mixing entropy depends on the number of independent kinetic units, i.e. solvent molecules and polymer segments. This alters the value of the interaction parameter, χ, as determined from experimental data.

D. Parameterization. All of the physical and chemical characteristics of the polymer–solvent–surface system are contained in eight model parameters: T, l, Z_p, $\bar{V}_p$, $\bar{V}_s$, φ_k^b, χ, and χ_s. Values of these parameters must be determined from experimental conditions and component properties if the predictions of the model are to be validated.

The identification of the number of segments per polymer chain, Z_p, distinguishes the present model from lattice models[12] and earlier continuum models.[11,16] We require that the real polymer molecule and the idealized chain of segments have the same extended length and mean-squared end-to-end distance $\langle r^2\rangle_0$ (or radius of gyration $R_g = (\langle r^2\rangle_0/6)^{1/2}$). Thus we have

$$Z_p l = n_b l_b \quad (37)$$

and

$$Z_p l^2 = \langle r^2\rangle_0 = C_\infty n_b l_b^2 \quad (38)$$

where n_b is the number of backbone bonds per molecule and l_b is the average length per bond. The second equality in eq 38 defines the characteristic ratio C_∞ which depends on the polymer–solvent pair. Values of C_∞ are tabulated[29] or may be calculated from measured radii of gyration. Equations 37 and 38 are easily solved for

$$l = C_\infty l_b \quad (39)$$

and

$$Z_p = \frac{n_b}{C_\infty} = \frac{bM_p}{M_m C_\infty} \quad (40)$$

where M_p and M_m are the polymer and monomer molecular weights and b is the number of backbone bonds per monomer.

Suppose that m_k° and m_k^b are the mass densities of component k in pure state and in bulk solution. Partial molar volumes are given by

$$\bar{V}_p = \frac{M_m}{m_p^\circ}, \qquad \bar{V}_s = \frac{M_s}{m_s^\circ} \quad (41)$$

for polymer (monomer basis) and solvent. Molar densities and volume fractions in bulk solution are easily calculated as $\rho_p^b = m_p^b/M_m$ and $\varphi_p^b = \bar{V}_p\rho_p^b$ with corresponding equations for solvent or other components.

The parameter characterizing polymer–solvent interaction depends on the selected equation of state. Values of the Flory–Huggins χ parameter are quoted in the literature for many polymer–solvent pairs; however, these values are appropriate insofar as the usual form of the Flory–Huggins equation assumes equal partial molar volumes of monomers and solvent molecules. For the extended Flory–Huggins equation described in the previous section, we determine the temperature dependence of χ and the Theta temperature T_θ (at which $\chi = 0.5$) from measurements of the molecular weight dependence of the

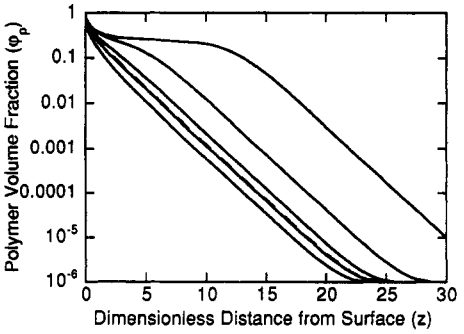

Figure 1. Volume fraction of polymer as a function of the dimensionless distance from an adsorbing surface. Solid curves (left to right): χ = 0.40, 0.50, 0.55, 0.57, and 0.60, respectively; other parameters include χ_s = 1.0, Z_p = 1000, $\varphi_p^b = 1.0 \times 10^{-6}$, and $\bar{V}_s/\bar{V}_p = 1.0$. Dashed curve: χ_s = 1.5 and χ = 0.50 with other parameters the same.

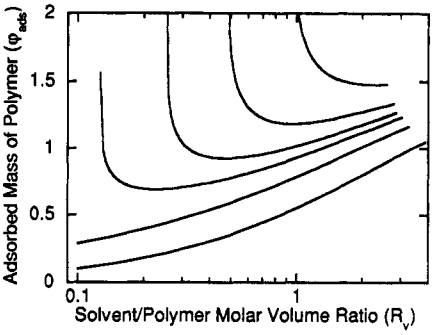

Figure 2. Effect of the solvent/polymer molar volume ratio $R_v \equiv \bar{V}_s/\bar{V}_p$ upon the dimensionless adsorbed mass of polymer. Curves from bottom to top are for χ = 0.40, 0.50, 0.535, 0.57, and 0.60, respectively. Other parameters include χ_s = 1.0, Z_p = 1000, and $\varphi_p^b = 1.0 \times 10^{-6}$.

critical temperature of the polymer–solvent binodal curve. Utilizing eqs 34 and 35, a Schultz–Flory plot[30] yields values of T_θ and the entropy parameter ψ_1 which determine χ through

$$\chi = \frac{1}{2} - \psi_1\left(1 - \frac{T}{T_\theta}\right) \tag{42}$$

The relative adsorption energy, χ_s, is difficult to characterize and is usually left as undetermined. Recently, displacement experiments[31] have determined χ_s values for several systems. We utilize these values in some of the calculations reported here. The predictions of the present model, as well as those of the Scheutjens–Fleer lattice model,[12] are not sensitive to the value of χ_s as long as the total segment–surface adsorption energy per polymer molecule is much greater than kT.

IV. Adsorption at a Single Surface

In this section we will present selected calculations which illustrate the dependence of polymer layer structure on polymer–solvent interactions and molecular volume differences. Then, we will compare model predictions with experimental data for polystyrene (PS) adsorbing from cyclohexane (CH) and CCl_4 onto silica and chrome surfaces.

A. Solvent Quality and Molecular Volume Effects. Figure 1 shows the variation of polymer volume fraction $\varphi_p(z)$ with dimensionless distance from an adsorbing surface for several values of the polymer–solvent interaction parameter, χ. For good ($\chi < 0.5$) and Theta (χ = 0.5) solvents, the decrease in $\varphi_p(z)$ is approximately exponential except in the vicinity of the surface and where the profile merges into bulk solution. The polymer distribution becomes noticably nonexponential in poor solvents ($\chi > 0.5$). As the binodal phase boundary is approached (increasing χ, decreasing T), a relatively thick layer of concentrated polymer builds up near the surface. The free energy contribution of polymer–solvent interactions becomes more positive as χ increases. The system thus minimizes its free energy by adsorbing more polymer under poorer solvent conditions.

Polymer volume fraction profiles for χ_s = 1.0 and 1.5 (both for χ = 0.5), also shown in Figure 1, nearly superimpose. The surface coverage $\varphi_0 \equiv \varphi_p(0)$ and φ_{ads} reach limiting values as χ_s increases above 1.0. Similar trends are predicted by the Scheutjens–Fleer lattice model.[12] In general, the predicted structure of adsorbed layers is insensitive to χ_s for values greater than the thermal energy kT per adsorbed segment.

Unlike the polymer volume fraction profile, values of φ_{ads}, defined by eq 33, are readily measured using several experimental methods. Figure 2 illustrates the effect of χ and unequal partial molar volumes upon φ_{ads}. The value of φ_{ads} increases with χ as expected. In Theta or better solvents ($\chi \leq 0.5$), φ_{ads} increases with increasing partial molar volume ratio $R_v \equiv \bar{V}_s/\bar{V}_p$. However, in poor solvents, φ_{ads} exhibits a minimum at values of R_v which vary with χ.

The predicted variations in φ_{ads} with χ and R_v can be rationalized by considering the enthalpic and entropic contributions to the free energy densities a_h (eq 34) and Δa (eq 36). Polymer adsorption occurs because polymer–surface contacts lower the free energy of the system. However, adsorption entails some demixing of the polymer–solvent mixture; the measure of the free energy penalty associated with this demixing, Δa, includes enthalpic and entropic contributions. In the form of a_h given by eq 34, the positive enthalpic contribution $\chi\rho_s\varphi_p$ always favors polymer–solvent demixing and adsorption, but the negative entropic terms favor mixing and discourage adsorption.

Rationalization of the mixing free energy density Δa, eq 36, aids interpretation of the results in Figure 2. We expect Δa to be positive if the adsorbed polymer layer is assembled from an equilibrium state of the bulk solution. A Taylor series expansion of eq 36 in powers of $\varphi_p - \varphi_p^b$ gives

$$\bar{V}_p\Delta a \approx \frac{1}{2}\left[\frac{1}{R_v(1-\varphi_p^b)} + \frac{1}{Z_p\varphi_p^b} - \frac{2\chi}{R_v}\right](\varphi_p - \varphi_p^b)^2 + \frac{1}{6}\left[\frac{1}{R_v(1-\varphi_p^b)^2} - \frac{1}{Z_p(\varphi_p^b)^2}\right](\varphi_p - \varphi_p^b)^3 + O((\varphi_p - \varphi_p^b)^4) + \cdots \tag{43}$$

The enthalpic contribution is $-2\chi/R_v$ which appears in the coefficient of $(\varphi_p - \varphi_p^b)^2$. If we take, for the moment, $Z_p\varphi_p^b \gg 1$ and $\varphi_p^b \ll 1$, then the coefficient of $(\varphi_p - \varphi_p^b)^2$ is $(0.5 - \chi)/R_v$. This coefficient is positive and disfavors adsorption for values of $\chi < 0.5$. If $\chi > 0.5$, the coefficient is negative (favorable for adsorption) and can become large as R_v decreases. Thus, for poor solevnts, adsorption eventually increases as R_v decreases as seen in Figure 2.

Except for $-2\chi/R_v$, all of the other terms depending on R_v in eq 43 are positive entropic contributions. As R_v increases, these entropic terms become less important; hence adsorption eventually increases with R_v for all solvent conditions.

In more physical terms, R_v represents the ratio of the volume of a solvent molecule to that of a polymer segment. At constant volume fractions of polymer and solvent, decreasing R_v increases the number of solvent molecules

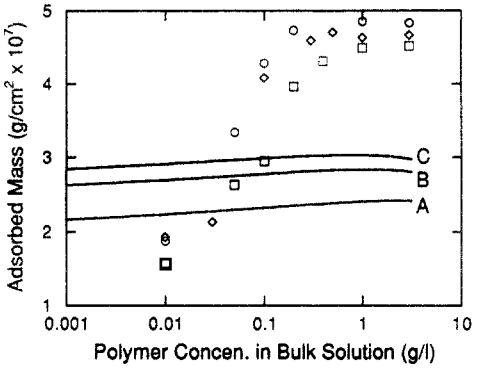

Figure 3. Experimental and calculated adsorption isotherms for PS adsorbing onto chrome surfaces from CH at 35 °C. Experimental data: PS molecular weights (g/mol) of 2.42×10^6 (squares), 7.62×10^6 (circles), and 1.34×10^7 (diamonds), all from ref 33. Corresponding calculated isotherms, curves A, B, and C, are for Z_p = 4210, 13240, and 23290, respectively. Other parameters include $\chi_s = 1.5$, $\chi = 0.496$, $\bar{V}_p = 99.1$ g/cm³, and $\bar{V}_s = 108.0$ g/cm³.

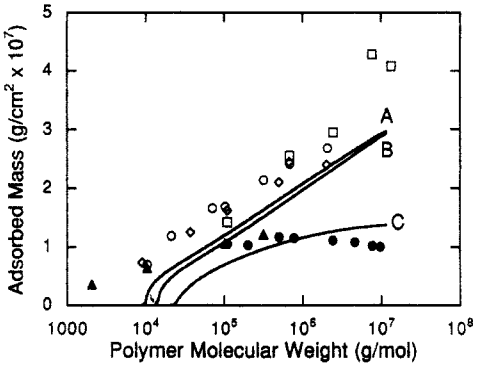

Figure 4. Experimental and calculated values of the polymer adsorbed mass per area, at 35 °C, as a function of polymer molecular weight. Experimental data are for adsorption of PS from CH onto chrome (squares, ref 33, $m_p^b = 0.1$ g/L), from CH onto silica (diamonds, ref 37, 0.3 g/L; open circles, ref 38, 1.48 g/L), from CCl_4 onto chrome (filled circles, ref 35, 1.0 g/L), and from CCl_4 onto silica (filled triangles, ref 37, 0.74 g/L). Curves A and B are calculated adsorbed masses for adsorption from CH and utilize $\varphi_p^b = 1.48 \times 10^{-3}$ and 9.53×10^{-5}; also $\chi_s = 1.5$, $\chi = 0.496$, $\bar{V}_p = 99.1$ g/cm³, and $\bar{V}_s = 108.0$ g/cm³. Curve C is the calculated adsorbed mass from CCl_4; also $\chi_s = 1.0$, $\chi = 0.396$, $\varphi_p^b = 9.53 \times 10^{-4}$, $\bar{V}_p = 99.1$ g/cm³, and $\bar{V}_s = 96.5$ g/cm³.

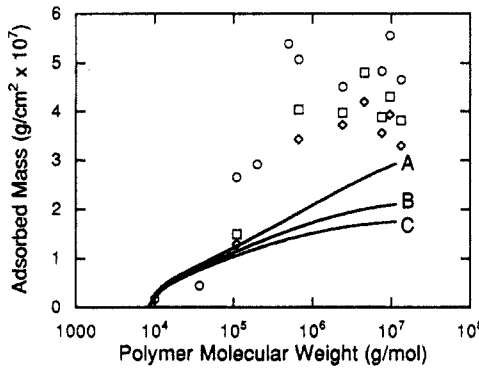

Figure 5. Experimental and calculated values of the polymer adsorbed mass as a function of polymer molecular weight. Experimental data are for adsorption of PS from CH onto chrome at 35 °C (circles, ref 33), 40 °C (squares, refs 34 and 36), and 45 °C (diamonds, refs 34 and 36). All data are for $m_p^b = 3.0$ g/L. The corresponding calculated values, curves A, B, and C, utilize $\chi = 0.496$, 0.456, and 0.416, respectively; also $\chi_s = 1.5$, $\varphi_p^b = 2.86 \times 10^{-3}$, $\bar{V}_p = 99.1$ g/cm³, and $\bar{V}_s = 108.0$ g/cm³.

per segment and therefore increases the entropy of mixing in bulk solution. If the latter is relatively high, then so is the entropy penalty which disfavors adsorption, so φ_{ads} decreases with decreasing R_v. In poor solvents, though, increasing the number of solvent molecules per segment also raises the number of polymer–solvent contacts and increases the free energy. Eventually, as R_v decreases, it becomes energetically favorable to form more polymer–polymer contacts by increasing φ_{ads}.

B. Comparisons with Experimental Data. Before presenting comparisons with experimental data, we discuss the parameterization of the PS–CH system. PS has two backbone bonds per monomer with an average length of 0.154 nm. The monomer molecular weight and polymer density are 104 g/mol and 1.05 g/cm³. The corresponding values for CH are 84.2 g/mol and 0.78 g/cm³. The accepted value[10] of T_θ for PS–CH solutions is 307.7 K. We obtain $\psi_1 = 2.590$ from PS–CH solution data[30] by constructing a Schultz–Flory plot as discussed earlier. For most Theta solvents,[32] the radius of gyration of PS is given by $R_g = 0.0290$ (nm/(g/mol)$^{1/2}$)$M_p^{1/2}$. Lastly, van der Beek[31] has reported χ_s values of 1.9 and 1.0 for PS adsorption from CH and CCl_4 onto silica.

These data and eqs 37–42 lead to the following model parameters for PS–CH: $l = 1.70$ nm, $Z_p = 0.00174$ (mol/g)M_p, $\bar{V}_p = 99.1$ cm³/mol, $\bar{V}_s = 108.0$ cm³/mol, and $\varphi_p^b = 0.953$ (cm³/g)m_p^b. At $T = 35.0$ °C, eq 42 gives $\chi = 0.496$. We use $\chi_s = 1.5$ instead of the reported value[31] of 1.9 due to numerical difficulties which arise when the volume fraction of polymer at $z = 0$ exceeds 0.9999. We have shown in Figure 1 that the predictions of the model become insensitive to χ_s for values greater than about 1.5.

The mass of polymer adsorbed at the surface per unit area, Γ, is the integral of the difference between the local mass density, $m_p(z)$, and that in bulk solution, m_p^b. The dimensionless adsorbed mass per area, φ_{ads}, is related to Γ by $\varphi_{ads} = \Gamma \bar{V}_p / l M_m$.

Many experiments demonstrate that Γ increases with m_p^b. Figure 3 shows experimental[33] and calculated adsorption isotherms for PS adsorbing from CH onto chrome at 35 °C. The experimental isotherms show that Γ increases steeply at first and then reaches a plateau value as m_p^b is increased. However, the data are not entirely consistent with other experiments[37,38] and earlier models[12,40] which show that the polymer adsorbed mass increases with molecular weight: in Figure 3, the adsorbed mass for 1.34×10^7 g/mol PS is less than that for 7.62×10^6 g/mol PS. The calculated values of Γ increase gradually with m_p^b; poor predictions of Γ are obtained for low and high values of m_p^b. The predicted values of Γ do increase with molecular weight as expected.

The differences between predicted and experimental adsorption isotherms cannot be ascribed to a single cause. At low values of m_p^b, the chemical potential of polymer in solution is overestimated by the Flory–Huggins equation-of-state, so the predicted adsorbed mass is too large, and the initial steepness of the adsorption isotherm is too gradual. At high values of m_p^b, the experiments may not yield equilibrium adsorbed layers. The neglect of "tails" in the regular perturbation expansion solution of the model equations may also be significant for the conditions of the experiments in Figure 3.

The variation of Γ with polymer molecular weight has been measured extensively using ellipsometry[33–36] or UV and IR spectroscopy combined with mass balances.[37,38] The measured values of Γ are compared with predictions of the present model in Figures 4 and 5. Figure 4 shows the molecular weight dependence of PS adsorbed mass at 35 °C, including data for adsorption from CH on chrome,[33] CH on silica,[37,38] CCl_4 on chrome,[35] and CCl_4 on silica.[37,38] At 35 °C, CH is essentially a Theta solvent for PS, and CCl_4 is a good solvent for PS. Lacking phase behavior

data for calculating a χ value for PS/CCl_4 at 35 °C, we employ a reported value[31] of $\chi = 0.396$ at 25 °C. We use $\chi_s = 1.5$ in the calculation for adsorption from CH onto silica and chrome, and $\chi_s = 1.0$ for adsorption[31] from CCl_4. Other parameters for the CCl_4 calculations are the same as for CH, except $\bar{V}_s = 96.5$ cm³/mol for CCl_4.

The data for PS adsorption from CH (Figure 4) is consistent between research groups for adsorption on silica[37,38] and with data for adsorption on chrome.[33] The measured value of Γ appears to increase logarithmically with PS molecular weight. The predicted values of Γ follow the same trend, although the values are roughly 5.0×10^{-8} g/cm² less than the experimental values over most of the molecular weight range. The two calculated curves for CH utilize values of φ_p^b which bracket the corresponding bulk solution concentrations used in the experiments.

The experimental data for adsorption from a good solvent, CCl_4 at 35 °C (Figure 4), first increase[37] and then become independent[35] of molecular weight. The predicted values of Γ follow the same qualitative trend. Although the quantitative agreement is satisfactory at higher molecular weights, the model fails at low molecular weight. The contribution of "tails" to the layer structure becomes more important for polymer molecular weights near the critical length for adsorption. The discrepancy between theory and experiment for low molecular weights is therefore probably due to the neglect of higher order terms in the perturbation series solution of eqs 23a–e.

The experimental data and calculations do not agree as well for adsorption from a more concentrated solution of PS in CH. The data in Figure 5 are for adsorption onto chrome[33,34,36] at 35, 40, and 45 °C. The corresponding χ values are 0.496, 0.456, and 0.416 as found from eq 42. Although the data display considerable scatter, values of Γ tend to be highest at 35 °C, lowest at 45 °C, and generally increasing with PS molecular weight. The predicted values of Γ also increase with temperature and molecular weight, but the numerical values are about half of the experimental values of Γ. The scatter in the data could be due to equilibration problems caused by the high PS molecular weight and the relatively high bulk solution concentration. The value for m_p^b was 3.0 g/L for the data in Figure 5 and is much higher than any of the incubation concentrations for the data in Figure 4. The level of agreement between experimental data and calculations in Figures 4 and 5 is satisfactory, considering the approximations of the model and the possibility that some of the polymer layers are not equilibrium structures.

Ellipsometric data[33] for the thickness of PS layers adsorbed from CH at 35 °C are compared with calculated thicknesses in Figure 6. Curves A ($m_p^b = 3.0$ g/L) and B ($m_p^b = 0.1$ g/L) are thicknesses calculated from the first moment of the polymer volume fraction profile. The thickness measured by ellipsometry should equal $2\Gamma_1/\Gamma_0$ for exponential polymer density profiles.[41] Here Γ_1 is the first moment (length × mass/area) and Γ_0 is the adsorbed mass per area. The thicknesses calculated from the first moment are substantially less than the experimental thicknesses. Decreasing the incubation concentration decreases the layer thicknesses observed in the experiments as well as those predicted from the model. However, measured thicknesses for PS adsorbed at higher temperatures (not shown) are slightly greater than those at 35 °C; the corresponding calculated thicknesses, on the contrary, are less than those predicted at 35 °C.

Dividing the polymer adsorbance by the layer thickness gives the average concentration of polymer in the layer. Average polymer concentrations derived from ellipsometric measurements[33] are also shown in Figure 6. Corresponding predictions from the present model are represented by curves C ($m_p^b = 3.0$ g/L) and D ($m_p^b = 0.1$ g/L). Although the calculated curves show the correct qualitative variation with molecular weight, the model clearly predicts much higher average polymer concentrations than are seen experimentally. Furthermore, decreasing the incubation concentration leads to increasing predicted average polymer concentrations; the opposite trend is seen in the experimental data.

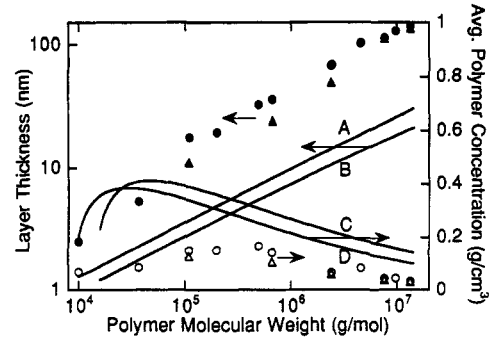

Figure 6. Experimental and calculated values of the polymer layer thickness and average polymer concentration, at 35 °C, as a function of polymer molecular weight. Experimental data are for adsorption of PS from CH onto chrome (ref 33). Curve A (calculated) and the filled circles (data) are thicknesses for $m_p^b = 3.0$ g/L; corresponding average polymer concentrations are given by curve D and the open circles. Curve B (calculated) and the filled triangles (data) are thicknesses for $m_p^b = 0.1$ g/L; corresponding average polymer concentrations are given by curve C and the open triangles. Parameters include $\chi_s = 1.5$, $\chi = 0.496$, $\varphi_p^b = 2.86 \times 10^{-3}$ or 9.53×10^{-4}, $\bar{V}_p = 99.1$ g/cm³, and $\bar{V}_s = 108.0$ g/cm³.

C. Discussion. The reasons for the disagreement between experiment and theory for layer thicknesses and average polymer concentrations are not clear, but several possible causes can be suggested. First, in the solution of the model equations, we truncate the perturbation expansion of $q(z,t)$ at the zero-order term, thus precluding polymer configurations which end at a point not on the surface ("tails"). This omission may be responsible for the low predictions of both Γ (for lower polymer molecular weights) and layer thickness.

Second, the extended form of the Flory–Huggins equation of state does not provide an accurate representation of the thermodynamics of real polymer–solvent interactions. This fact is reflected in the concentration and temperature dependence of χ observed for many systems. The model equations reported here, particularly eq 22, provide a prescription for incorporating more sophisticated polymer–solvent thermodynamics.

Last, some of the polymer layers studied in the ellipsometry experiments may not have been equilibrium structures. If substantial amounts of nonadsorbed polymer were entangled with polymer adsorbed on the surfaces, then higher adsorbances and layer thicknesses would be observed than an equilibrium model would predict. The equilibrium structure of a polymer layer would presumably be reached through sequential adsorption and collapse of polymer molecules in coiled solution configurations. Equilibration difficulties could therefore prevent the average polymer concentration from increasing to higher values during the collapse process. These questions certainly merit further study.

V. Conclusions

We have developed a continuum model for polymer adsorption, within the framework of self-consistent field

theory, which provides adequate predictions of polymer layer structure. Under some conditions, the agreement between predicted and experimental adsorbed masses per area is satisfactory, especially when the incubation concentration of polymer in bulk solution is not very high. All of the model parameters have been taken from experimental data; none have been adjusted to fit experimental results.

The present model differs from earlier continuum[40] and lattice-based[12] self-consistent field models in two important ways. First, the present model properly accounts for the inherent stiffness of polymer molecules by requiring that real molecules and idealized chains of segments have the same extended lengths and radii of gyration. This determines the number of segments per chain and has a critical effect upon the entropy of mixing chains and solvent. Second, the present model incorporates molecular volume effects by allowing the solvent and polymer segments to have different partial molar volumes. Both the entropy and enthalpy of mixing are influenced by molar volume differences. Accurate prediction of the polymer adsorbed mass requires the use of an equation of state which properly balances the entropy penalty associated with demixing with the enthalpy of polymer–solvent interactions. The enthalpic contribution depends on the number of solvent–monomer contacts, but the mixing entropy depends on the numbers of solvent molecules and polymer *segments*.

The results shown above, especially those in Figure 2, demonstrate that the structure of the polymer interphase is quite sensitive to the form of the equation of state, in this case provided by an extended form of Flory–Huggins theory. The importance of polymer chain length upon adsorption has long been understood,[12] but the consequences of differing molecular volumes have not been considered or appreciated. The results in Figure 2 imply that changes in the ratio of solvent to polymer molar volume can alter the polymer adsorbed mass significantly, often as much as that effected by changed in polymer molecular weight. The molar volume ratio could be utilized as a design parameter for controlling polymer adsorption.

The comparisons between polymer layer thicknesses measured by ellipsometry and calculated from the model are not satisfactory. The poor agreement may be due to the approximations invoked in the solution of the model equations. Specifically, the retention of only the zero-order term in the perturbation expansion of q in powers of $1/Z_p$ results in the neglect of chain end effects and omission of "tails" from the structure of the polymer layer. Similar shortcomings were found in previous calculations,[40a] but inclusion of end effects via a matched asymptotic solution[40b] produced model predictions that were in better agreement with experimental thickness measurements. In the present model, the utility of including higher order terms for predicting interphase thicknesses has not yet been demonstrated.

With regard to forces between adsorbed polymer layers, experiments[10] and earlier models[12] have demonstrated that the adsorbed mass, rather than the layer thickness, is the key feature which influences the details of polymeric interlayer interactions. The utility of the present model for predicting forces between adsorbed layers will be demonstrated in a subsequent publication.[18]

Acknowledgment. This work was supported by the State of Texas through the Engineering Excellence Fund at Texas A&M University, the National Science Foundation (Grants CTS-9009754 and CTS-9258137), and a Young Faculty Grant from the Du Pont Co.

References and Notes

(1) Flory, P. J. *Statistical Mechanics of Chain Molecules*; Hanser: Munich, 1989.
(2) de Gennes, P. G. *Scaling Concepts in Polymer Physics*; Cornell University: Ithaca, NY, 1979.
(3) For polymer which is adsorbed, grafted, or otherwise tethered at a phase boundary, the length scale of inhomogeneity is much greater than that of interfaces separating phases containing small molecules. Hence the term "interphase" is an apt description of the region in which the polymer distribution is inhomogeneous.
(4) Ploehn, H. J.; Russel, W. B. *Adv. Chem. Eng.* **1990**, *15*, 137.
(5) Cahn, J.; Hilliard, J. E. *J. Chem. Phys.* **1958**, *28*, 258. Cahn, J. *J. Chem. Phys.* **1977**, *66*, 3667. Widom, B. *Physica A* **1979**, *95*, 1.
(6) de Gennes, P. G. *Macromolecules* **1981**, *14*, 1637; *Macromolecules* **1982**, *15*, 492.
(7) Klein, J.; Pincus, P. *Macromolecules* **1982**, *15*, 1129.
(8) Rossi, G.; Pincus, P. *Europhys. Lett.* **1988**, *5*, 641. Rossi, G.; Pincus, P. *Macromolecules* **1989**, *22*, 276.
(9) Ingersent, K.; Klein, J.; Pincus, P. *Macromolecules* **1990**, *23*, 548.
(10) Patel, S. S.; Tirrell, M. *Annu. Rev. Phys. Chem.* **1989**, *40*, 597.
(11) Hong, K. M.; Noolandi, J. *Macromolecules* **1981**, *14*, 727.
(12) Scheutjens, J. M. H. M.; Fleer, G. J. *J. Phys. Chem.* **1979**, *83*, 1619. Scheutjens, J. M. H. M.; Fleer, G. J. *J. Phys. Chem.* **1980**, *84*, 178. Scheutjens, J. M. H. M.; Fleer, G. J. *Macromolecules* **1985**, *18*, 1882.
(13) Edwards, S. F. *Proc. R. Soc. London* **1965**, *85*, 613.
(14) Freed, K. F. *Adv. Chem. Phys.* **1972**, *22*, 1.
(15) Helfand, E. *J. Chem. Phys.* **1975**, *62*, 999.
(16) Helfand, E.; Sapse, A. M. *J. Polym. Sci., Polym. Symp.* **1976**, *54*, 289.
(17) Evans, E.; Needham, D. *Macromolecules* **1988**, *21*, 1823. Evans, E. *Macromolecules* **1989**, *22*, 2277.
(18) Ploehn, H. J. *Macromolecules*, following paper in this issue.
(19) McQuarrie, D. A. *Statistical Mechanics*; Harper & Row: New York, 1976.
(20) Eyring, H.; Henderson, D.; Stover, B. J.; Eyring, E. M. *Statistical Mechanics and Dynamics*; Wiley: New York, 1964.
(21) Kirkwood, J. G.; Buff, F. P. *J. Chem. Phys.* **1949**, *17*, 338.
(22) Lyklema, J. *Fundamentals of Interface and Colloid Science, Vol. 1: Fundamentals*; Academic: London, 1991.
(23) Mackor, E. L. *J. Colloid Sci.* **1951**, *6*, 492. Mackor, E. L.; van der Waals, J. H. *J. Colloid Sci.* **1952**, *7*, 535.
(24) Ash, S. G.; Everett, D. H.; Radke, C. J. *J. Chem. Soc., Faraday Trans. 2* **1973**, *69*, 1256.
(25) Everett, D. H. *Faraday Discuss. Chem. Soc.* **1978**, *65*, 215.
(26) Everett, D. H. *Pure Appl. Chem.* **1972**, *31*, 579.
(27) Verwey, E. J. W.; Overbeek, J. Th. G. *Theory of the Stability of Lyophobic Colloids*; Elsevier: Amsterdam, 1948.
(28) de Gennes, P. G. *Adv. Colloid Interface Sci.* **1987**, *27*, 189.
(29) Brandrup, J.; Immergut, E. H. *Polymer Handbook*; Wiley: New York, 1975.
(30) Schultz, A. R.; Flory, P. J. *J. Am. Chem. Soc.* **1952**, *74*, 4760.
(31) van der Beek, G. Ph.D. Dissertation, Wageningen Agricultural University, 1991.
(32) Schmidt, M.; Burchard, W. *Macromolecules* **1981**, *14*, 210.
(33) Takahashi, A.; Kawaguchi, M.; Hirota, H.; Kato, T. *Macromolecules* **1980**, *13*, 884.
(34) Kawaguchi, M.; Takahashi, A. *J. Polym. Sci.: Polym. Phys. Ed.* **1980**, *18*, 2069.
(35) Kawaguchi, M.; Hayakawa, K.; Takahashi, A. *Macromolecules* **1983**, *16*, 631.
(36) Kawaguchi, M.; Takahashi, A. *Macromolecules* **1983**, *16*, 1465.
(37) Vander Linden, C.; Van Leemput, R. *J. Colloid Interface Sci.* **1978**, *67*, 48.
(38) Kawaguchi, M.; Hayakawa, K.; Takahashi, A. *Polym. J.* **1980**, *12*, 265.
(39) Peck, D. G.; Johnston, K. P. *Macromolecules*, in press.
(40) Ploehn, H. J.; Russel, W. B.; Hall, C. K. *Macromolecules* **1988**, *21*, 1075. Ploehn, H. J.; Russel, W. B. *Macromolecules* **1989**, *22*, 266.
(41) Marques, C. M.; Frigerio, J. M.; Rivory, J. *J. Opt. Soc. Am. B* **1991**, *8*, 2523.